NASA TN D-947



# TECHNICAL NOTE

D-947

## WIND-TUNNEL TESTS OF SEVEN STATIC-PRESSURE PROBES AT TRANSONIC SPEEDS

By Francis J. Capone

Langley Research Center
Langley Field, Va.

NATIONAL AERONAUTICS AND SPACE ADMINISTRATION

WASHINGTON

November 1961

NATIONAL AERONAUTICS AND SPACE ADMINISTRATION

TECHNICAL NOTE D-947

# WIND-TUNNEL TESTS OF SEVEN STATIC-PRESSURE PROBES AT TRANSONIC SPEEDS

By Francis J. Capone



## SUMMARY

Wind-tunnel tests have been conducted to determine the errors of seven static-pressure probes mounted very close to the nose of a body of revolution simulating a missile forebody. The tests were conducted at Mach numbers from 0.80 to 1.08 and at angles of attack from -1.7° to 8.4°. The test Reynolds number per foot varied from $3.35 \times 10^6$ to $4.05 \times 10^6$. For three 4-vane, gimbaled probes, the static-pressure errors remained constant throughout the test angle-of-attack range for all Mach numbers except 1.02. For two single-vane, self-rotating probes having two orifices at ±37.5° from the plane of symmetry on the lower surface of the probe body, the static-pressure error varied as much as 1.5 percent of free-stream static pressure through the test angle-of-attack range for all Mach numbers. For two fixed, cone-cylinder probes of short length and large diameter, the static-pressure error varied over the test angle-of-attack range at constant Mach numbers as much as 8 to 10 percent of free-stream static pressure.

## INTRODUCTION

The Langley Research Center has conducted wind-tunnel tests to determine the errors, at angles of attack and at transonic speeds, of seven static-pressure probes (figs. 1 and 2) mounted very close to the nose of a body of revolution simulating a missile forebody.

Three of the probes were equipped with a gimbal system and four vanes that alined the probe with the local flow.

For two other probes, two static-pressure orifices were located at ±37.5° from the plane of symmetry on the lower surface of the probe to minimize the errors at angles of attack. In order to maintain the angle-of-attack compensation at angles of sideslip and at angles of roll in combination with angle of attack, the probes were designed to rotate about their longitudinal axis and were equipped with a single vane to keep the orifices alined with the cross-flow component of the local velocity.

Two probes were fixed, cone-cylinder probes of short length and large diameter which previous tests (ref. 1) had shown to be relatively insensitive to inclination through a small (5°) range of angle of attack at supersonic speeds. Although the errors of these probes at supersonic speeds were large (on the order of 21 percent of the static pressure), the percentage errors were constant over a large Mach number range and were, therefore, considered satisfactory for the barometric mission for which the probes were designed.

The tests of the probes covered a Mach number range of 0.80 to 1.08 and an angle-of-attack range of -1.7° to 8.4°. The test Reynolds number per foot varied from $3.35 \times 10^6$ to $4.05 \times 10^6$.



## SYMBOLS

| | |
|---|---|
| D | maximum diameter of body, 20.78 in. |
| M | free-stream Mach number |
| p | local static pressure sensed by probe, lb/sq ft |
| $p_\infty$ | free-stream static pressure, lb/sq ft |
| r | local radius of body, in. |
| r' | local radius of probe, in. |
| x | axial distance from theoretical body nose, positive forward from nose, in. |
| x' | axial distances from tip of probe, positive rearward from tip, in. |
| $\alpha$ | body angle of attack, deg |
| $\theta$ | maximum angular range of probe in vertical plane, deg |
| $\psi$ | maximum angular range of probe in horizontal plane, deg |

## MODELS

### Probes

Probes A, B, and C.- Sketches of probes A, B, and C are given in figures 1(a) and (b) and photographs are given as figures 2(a), (b), and (c).

These probes were designed to eliminate the static-pressure error due to angles of attack and sideslip by use of a gimbal mechanism similar to the one described in reference 2 and four vanes for stabilization. Probes A and C were mass balanced about the center of rotation while probe B was not. There were three circumferential rows of eight orifices each for probes A and C and of four orifices each for probe B. All orifices were 0.05 inch in diameter. Probe A had a probe body with 1° taper with the middle orifice row located at $\frac{x}{D} = 0.358$ ahead of the theoretical nose of the body. Probe B, which was a half-size model of probe A, also had the same orifice location relative to the tip of the body. Probe C had a probe body with 1° taper with its middle orifice row located at $\frac{x}{D} = 0.397$. The vanes on probe C had diamond-shaped cross sections.



Probes D and E.- Sketches of these probes are given in figure 1(c) and photographs in figures 2(d) and (e). These probes were designed to compensate for errors due to angles of attack and sideslip and to angles of roll in combination with angles of attack. The radial position of the orifices (±37.5° from the plane of symmetry on the lower surface of the probe) is designed to compensate for the static-pressure error due to angle of attack. This orifice arrangement was based on data of reference 3.

In order to maintain the angle-of-attack compensation at angles of sideslip and at angles of roll in combination with angles of attack, the probes were equipped with a single vane at the rear of the probe body and a system of bearings that allowed the probe to rotate about its own roll axis. "O" rings were used to prevent leakage in the pressure transfer between the rotating probe and the tubing in the missile body.

Probe D had a 1.2° taper. The two orifices, having 0.042-inch diameters, were located at $\frac{x}{D} = 0.082$ ahead of the body. Probe E had a curved probe body. The two orifices (0.060-inch diameter) were located at $\frac{x}{D} = 0.057$.

Probes F and G.- Sketches of probes F and G are shown in figure 1(d) and photographs in figures 2(f) and (g). These probes were short, large-diameter probes having conical nose shapes (called "stubby" probes in ref. 1). The orifice arrangement consisted of a single circumferential row of 20 orifices of 0.04-inch diameter. The orifices were located a short distance behind the shoulder of the cone and slightly aft of the theoretical tip of the body of revolution.

Probe F had a maximum diameter of 1.50 inches, with a 25° conical nose, and orifices located at $\frac{x}{D} = -0.115$ aft of the theoretical tip

of the body. This probe was similar to that in reference 1. Probe G had a maximum diameter of 2.00 inches, with a 50° conical nose, and orifices located at $\frac{x}{D} = -0.121$ aft of the theoretical tip of the body. This probe was the same as the one tested in reference 1.

## Body

The probes were mounted on a body of revolution, whose shape is defined by the coordinates of figure 3. The length of the body from the theoretical tip to the point of attachment in the wind tunnel (beginning of 5° cone fairing) was 94 inches. As shown in figure 3, the rear portion of the body terminated in a cylindrical section having a diameter of 20.78 inches. The probes were attached to the body by use of adapters having a shape defined by coordinates given in figure 3. A photograph of the body with probe C is shown as figure 4.

L 1 5 6 3

## APPARATUS AND ACCURACIES

The present investigation was conducted in the Langley 16-foot transonic tunnel, which is a single-return atmospheric wind tunnel with a slotted octagonal test section. The speed range of this tunnel is from a Mach number of 0.20 to 1.10, with the Mach number being varied over this range by a variation of tunnel drive power. The body pivoted in such a manner that a point on the body (labeled axis of rotation in fig. 3) was kept on or near the tunnel center line throughout the angle-of-attack range.

A differential pressure gage was used to measure the difference between the static pressure sensed by the probe and the tunnel tank static pressure. Free-stream static pressure was determined from a calibration of the tunnel tank static pressure. Mach number was determined from a calibration of the difference between tunnel stagnation pressure and tunnel tank static pressure. A pendulum-type strain-gage inclinometer was located inside the body in order to determine the angle of attack.

The accuracies of these measurements have been estimated to be:

| | |
|---|---|
| $\frac{p - p_\infty}{p_\infty}$ | ±0.005 |
| M | ±0.003 |
| $\alpha$, deg | ±0.10 |

## RESULTS AND DISCUSSION

The results of the tests of the seven static-pressure probes are presented in figures 5 to 11. For each probe the variation of the static-pressure error coefficient $\frac{p - p_\infty}{p_\infty}$ with angle of attack is given for constant Mach numbers and the variation of $\frac{p - p_\infty}{p_\infty}$ with Mach number is given for $\alpha = 0^\circ$.



### Gimbaled Probes A, B, and C

The variation of static-pressure error coefficient with angle of attack at constant Mach numbers is presented in figures 5(a), 6(a), and 7(a) for probes A, B, and C. These figures show that, with the exception of probe B at $M = 1.02$, there is essentially no variation of $\frac{p - p_\infty}{p_\infty}$ with $\alpha$ for angles of attack from $-1.7^\circ$ to $8.4^\circ$, a range that is well within the angular range of each of the probes. The small (1 percent of free-stream static pressure) variation of $\frac{p - p_\infty}{p_\infty}$ with $\alpha$ for probe B at $M = 1.02$, a Mach number at which the body bow shock wave is just ahead of the probe orifices, is probably due to small variations in the position of the shock wave with changing angle of attack of the body.

The variation of static-pressure error coefficient $\frac{p - p_\infty}{p_\infty}$ with Mach number at $\alpha = 0^\circ$ for probes A, B, and C is presented in figures 5(b), 6(b), and 7(b). An increasing positive pressure field ahead of the body with an increase in Mach number up to $M = 1.0$ is evidenced by the large increasing positive errors measured by the probe. For probes A and B (figs. 5(b) and 6(b)) the static-pressure error coefficient increased from about 0.031 at $M = 0.80$ to about 0.074 at $M = 1.00$.

At $M = 1.05$ the error coefficient decreases to -0.006 for probe A and to -0.010 for probe B; these values are the errors of the isolated probes. The fact that the error coefficients of probes A and B are essentially the same indicates that there is little effect in reducing the size of probe A by one-half. That the error coefficients of probe C - 0.031 for $M = 0.80$ to 0.060 for $M = 1.00$ - are slightly smaller than those of probes A and B is due to the fact that the orifices of probe C are a greater distance ahead of the body $\left(\frac{x}{D} = 0.397 \text{ for probe C as compared with } \frac{X}{D} = 0.358 \text{ for probes A and B}\right)$.

## Self-Rotating Probes D and E

The variation of static-pressure error $\frac{p - p_\infty}{p_\infty}$ with angle of attack is presented in figures 8(a) and 9(a) for probes D and E. For probe D the error coefficient is approximately constant with angle of attack for Mach numbers up to 1.00 but varies by about 1.0 percent of free-stream static pressure at the two low supersonic Mach numbers. For probe E the error coefficient increases with increasing angle of attack at each Mach number, the maximum variation being about 1.5 percent. The variation of the error coefficient with $\alpha$ for probe E is similar to that obtained with a 37.5° orifice arrangement on the nose of an ogive-shaped tube (ref. 4). As discussed in reference 4, an improvement of the angle-of-attack compensation of a curve-shaped probe could probably be realized by increasing the angular positions of the orifices. (See also refs. 5 and 6.)

The variation of $\frac{p - p_\infty}{p_\infty}$ with Mach number at $\alpha = 0°$ for probes D and E is presented in figures 8(b) and 9(b). As shown by these figures, the error coefficients of both probes increase from 0.05 at $M = 0.80$ to 0.10 at $M = 1.0$. At $M = 1.05$, however, the error coefficient of probe D is -0.008 whereas that of probe E is -0.037. Again, as for probes A, B, and C, these are errors representative of an isolated probe.

## Stubby Probes F and G

The variation of static-pressure error $\frac{p - p_\infty}{p_\infty}$ with angle of attack for probes F and G is presented in figures 10(a) and 11(a). For both of these probes the variation of the error over the angle-of-attack range is large; for probe F the error varied by as much as 10 percent of free-stream static pressure and for probe G the error varied by as much as 8 percent.

In the tests of reference 1 it was found that the error of a probe similar to probe F remained within 2 percent of free-stream static pressure from $\alpha = 0°$ to 5° at supersonic speeds. Figure 10(a) shows that the error of probe F remains within 2 percent of static pressure through an angle-of-attack range from 0° to 5° at $M = 0.80$, 1.05, and 1.08; at $M = 0.90$, 0.95, and 1.00 the error was as high as 4 percent for the same 5° angle-of-attack range. The tests of reference 1 also showed that the errors of a probe the same as probe G remained within 1.5 percent of free-stream static pressure from $\alpha = 0°$ to 5° at supersonic speeds. Figure 11(a) shows that the error of probe G remains within 1.5 percent through an angle-of-attack range from 0° to 5° for all Mach numbers between 0.80 and 1.08 with the exception of $M = 1.00$ where the errors are as high as 3 percent.

L 1 5 6 3

The variation of $\frac{p - p_\infty}{p_\infty}$ with Mach number at $\alpha = 0^\circ$ for probes F and G is presented in figures 10(b) and 11(b). These figures show that the error coefficient varies by very large amounts over the test Mach number range, that is, 24 percent of free-stream static pressure for probe F and 38 percent for probe G. Thus, the design concept of these probes as discussed in reference 1 (i.e., a willingness to accept a large error provided the error is a constant percent of the free-stream static pressure over the Mach number range of interest) cannot be extended from the supersonic to the subsonic speed range.



## CONCLUSIONS

Wind-tunnel tests at transonic speeds of seven static-pressure probes mounted very close to the nose of a body of revolution at angles of attack of $-1.7^\circ$ to $8.4^\circ$ indicate the following:

1. For three 4-vane, gimbaled probes, the static-pressure errors remained constant throughout the test angle-of-attack range for all Mach numbers except 1.02. At a body angle of attack of $0^\circ$, the errors of the three probes increased from about 3 percent of free-stream static pressure at a Mach number of 0.80 to about 6 to 7 percent at a Mach number of 1.00.

2. For two single-vane, self-rotating probes having two orifices at $\pm 37.5^\circ$ from the plane of symmetry on the lower surface of the probe, the static-pressure error varied as much as 1.5 percent of free-stream static pressure through the test angle-of-attack range for all Mach numbers. At an angle of attack of $0^\circ$, the errors of both probes increased from 5 percent of free-stream static pressure at a Mach number of 0.80 to 10 percent at a Mach number of 1.00.

3. For two fixed, cone-cylinder probes of short length and large diameter, the static-pressure error varied over the test angle-of-attack range at constant Mach numbers as much as 8 to 10 percent of free-stream static pressure. At an angle of attack of $0^\circ$, the variation of the error over the Mach number range was 24 percent of free-stream static pressure for one probe and 38 percent for the other.

Langley Research Center,
National Aeronautics and Space Administration,
Langley Field, Va., June 30, 1961.

## REFERENCES

1. Vaughn, H. R., Barton, W. R., and Bennett, M. D.: Theoretical and Wind-Tunnel Calibration of Two Sandia Corporation Stubby Probes for Barometric Fuzing. SC-4304(TR), Sandia Corp. (Albuquerque, N. Mex.), May 1959.

2. Vaughn, Harold, and Barton, W. R.: The Aerodynamics of the Sandia Self-Aligning Probe (XMC-620). SC-3934(TR), Sandia Corp. (Albuquerque, N. Mex.), Jan. 1957.

3. Ritchie, Virgil S.: Several Methods for Aerodynamic Reduction of Static-Pressure Sensing Errors for Aircraft at Subsonic, Near-Sonic, and Low Supersonic Speeds. NASA TR R-18, 1959.

4. Capone, Francis J.: Transonic Wind-Tunnel Tests of An Error-Compensated Static-Pressure Probe. NASA TN D-961, 1961.

5. Robinson, Harold L.: Pressures and Associated Aerodynamic and Load Characteristics for Two Bodies of Revolution at Transonic Speeds. NACA RM L53L28a, 1954.

6. Cooper, Morton, and Hamilton, Clyde V.: Orientation of Orifices on Bodies of Revolution for Determination of Stream Static Pressure at Supersonic Speeds. NACA TN 2592, 1952.

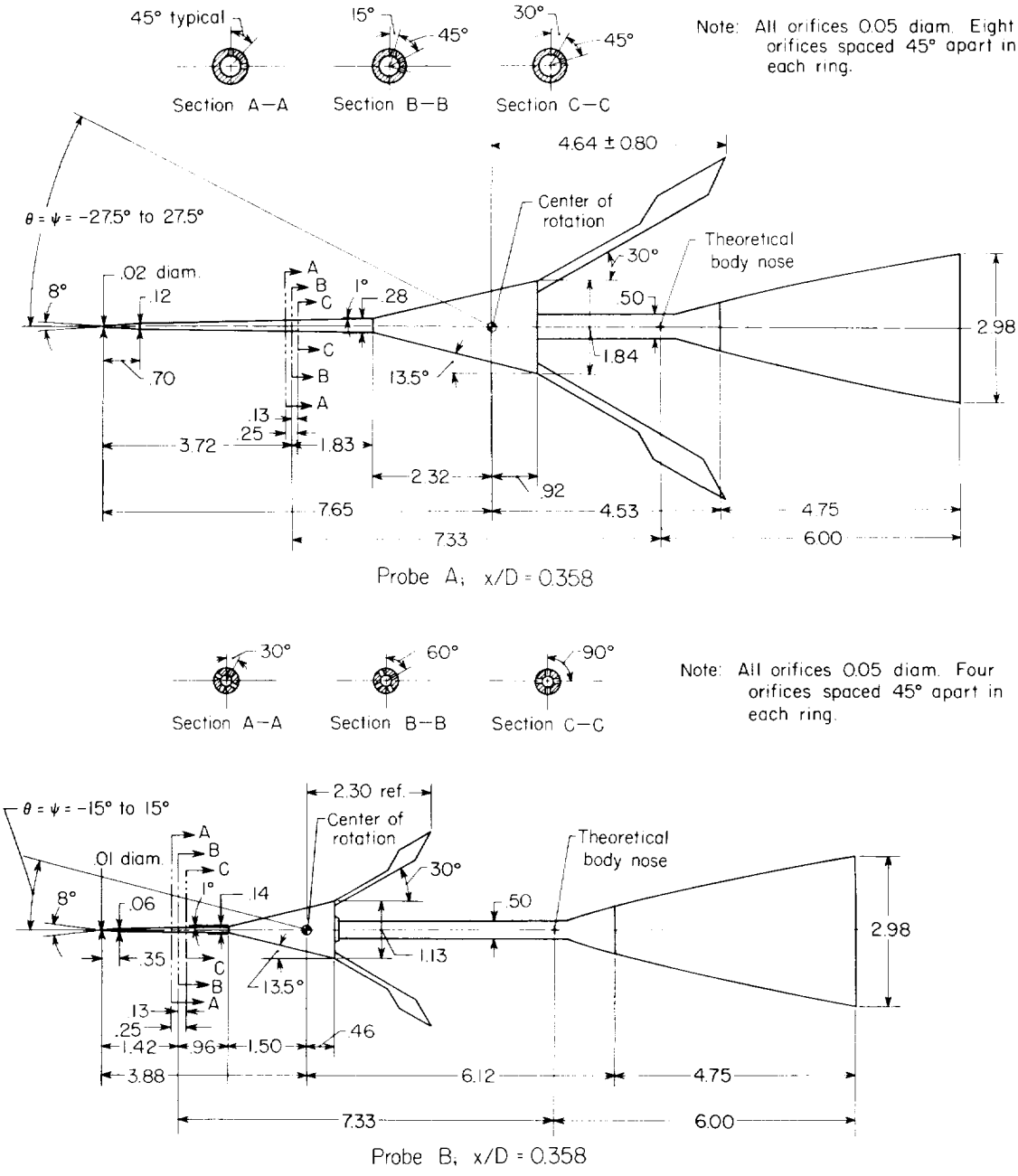


(a) Probes A and B.

Figure 1.- Sketches of the seven probes used during investigation. All dimensions are in inches unless otherwise noted.

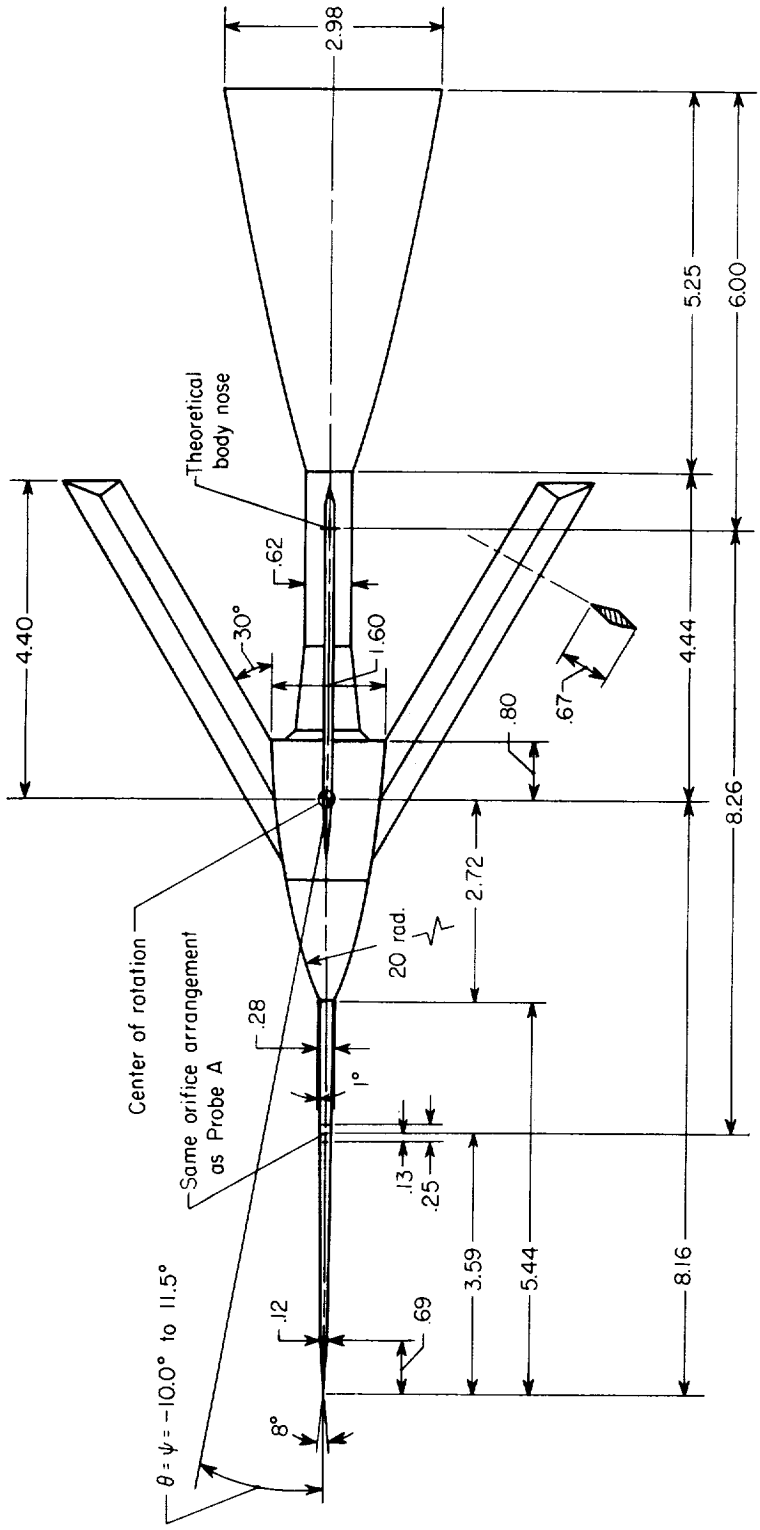


Probe C; x/D = 0.397

(b) Probe C.

Figure 1.- Continued.

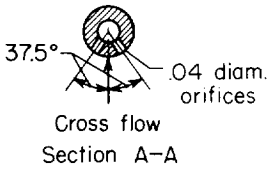


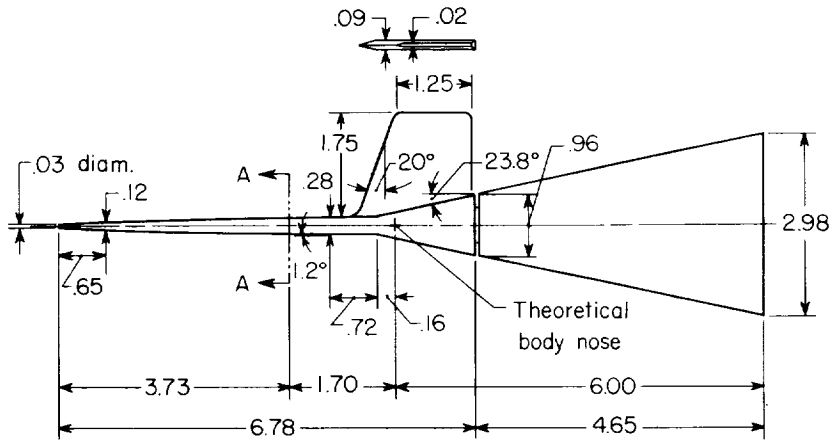


Probe D; x/D = 0.082

| Probe Coordinates | | | |
|---|---|---|---|
| x' | r' | x' | r' |
| 0.25 | 0.03 | 2.00 | 0.17 |
| .50 | .06 | 2.25 | .18 |
| .75 | .09 | 2.50 | .19 |
| 1.00 | .11 | 2.75 | .20 |
| 1.25 | .13 | 3.00 | .22 |
| 1.50 | .14 | 3.25 | .24 |
| 1.75 | .16 | 3.41 | .25 |

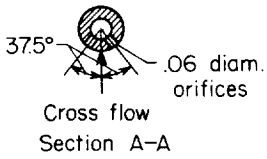


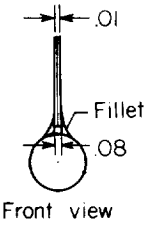


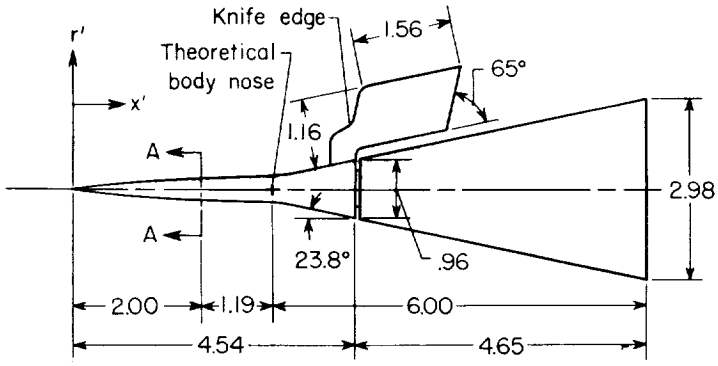


Probe E; x/D = 0.057

(c) Probes D and E.

Figure 1.- Continued

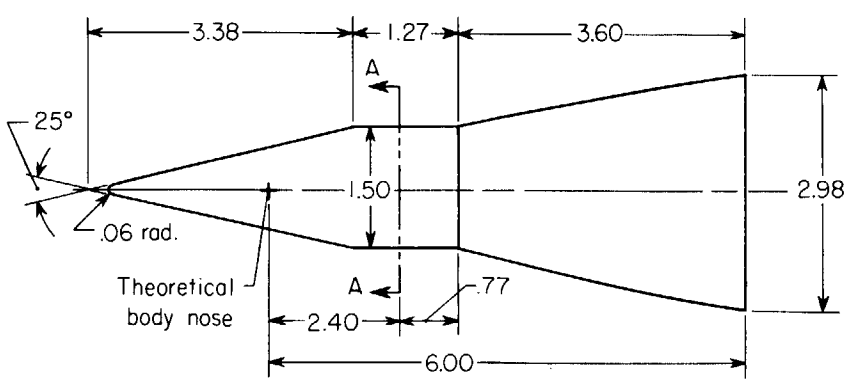


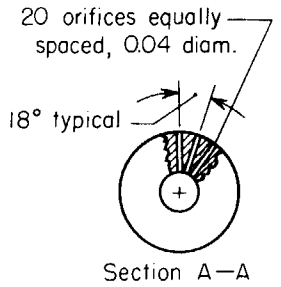


Probe F; x/D = -0.115

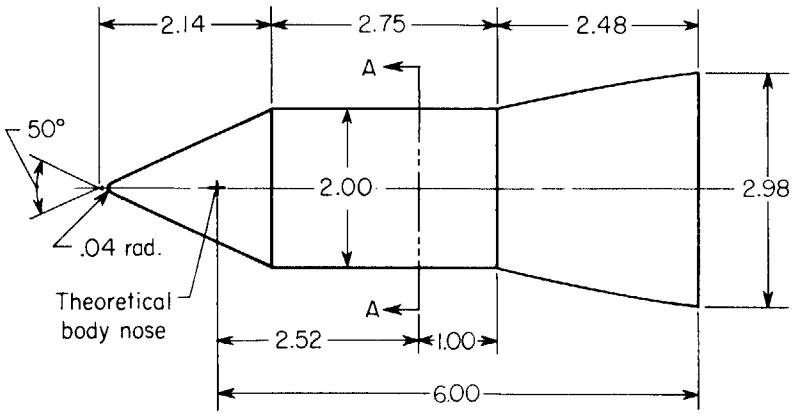


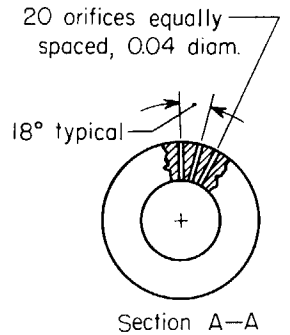


Probe G; x/D = -0.121

(d) Probes F and G.

Figure 1.- Concluded.

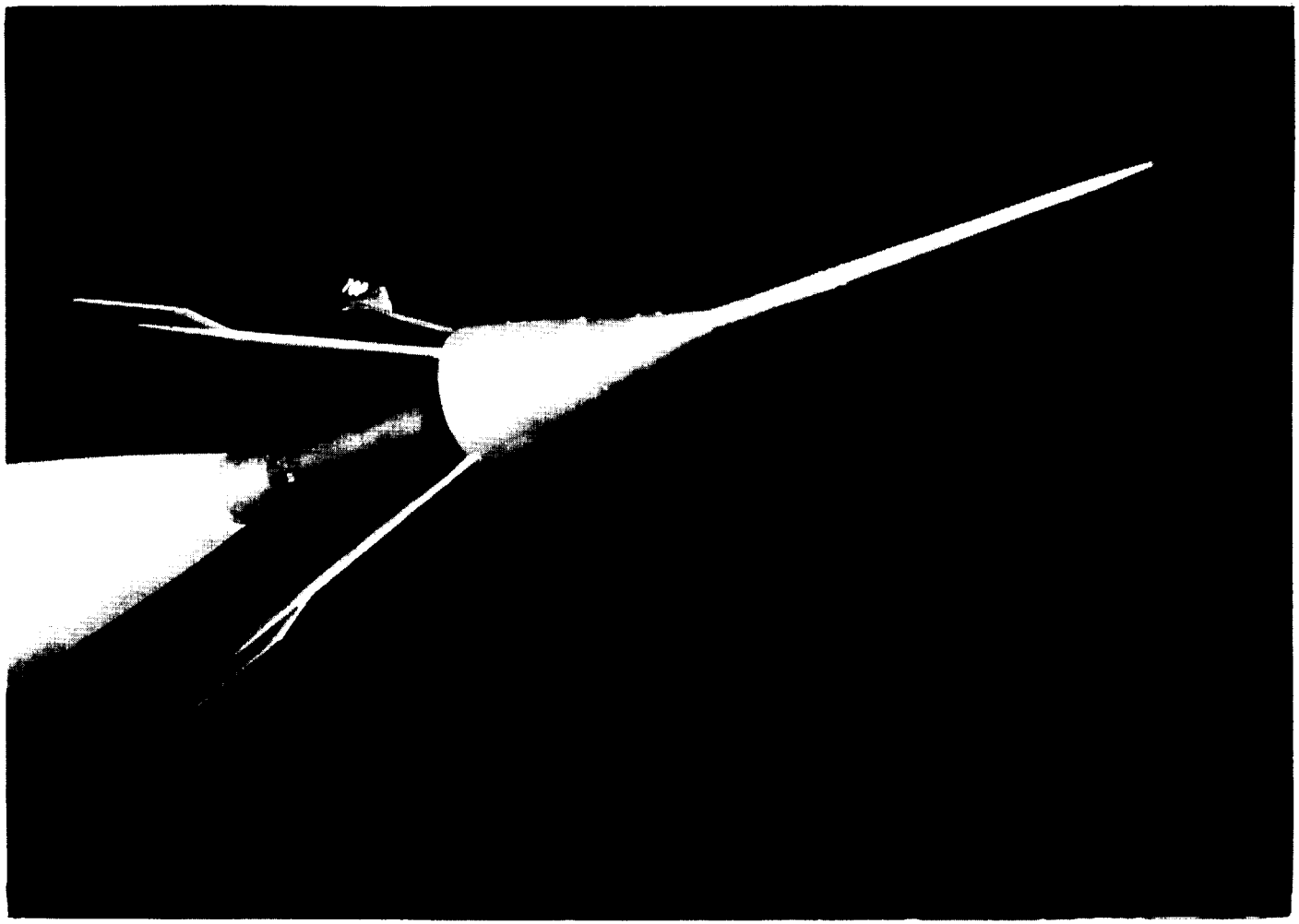

(a) Probe A. L-59-8048

Figure 2.- Photographs of the seven probes.

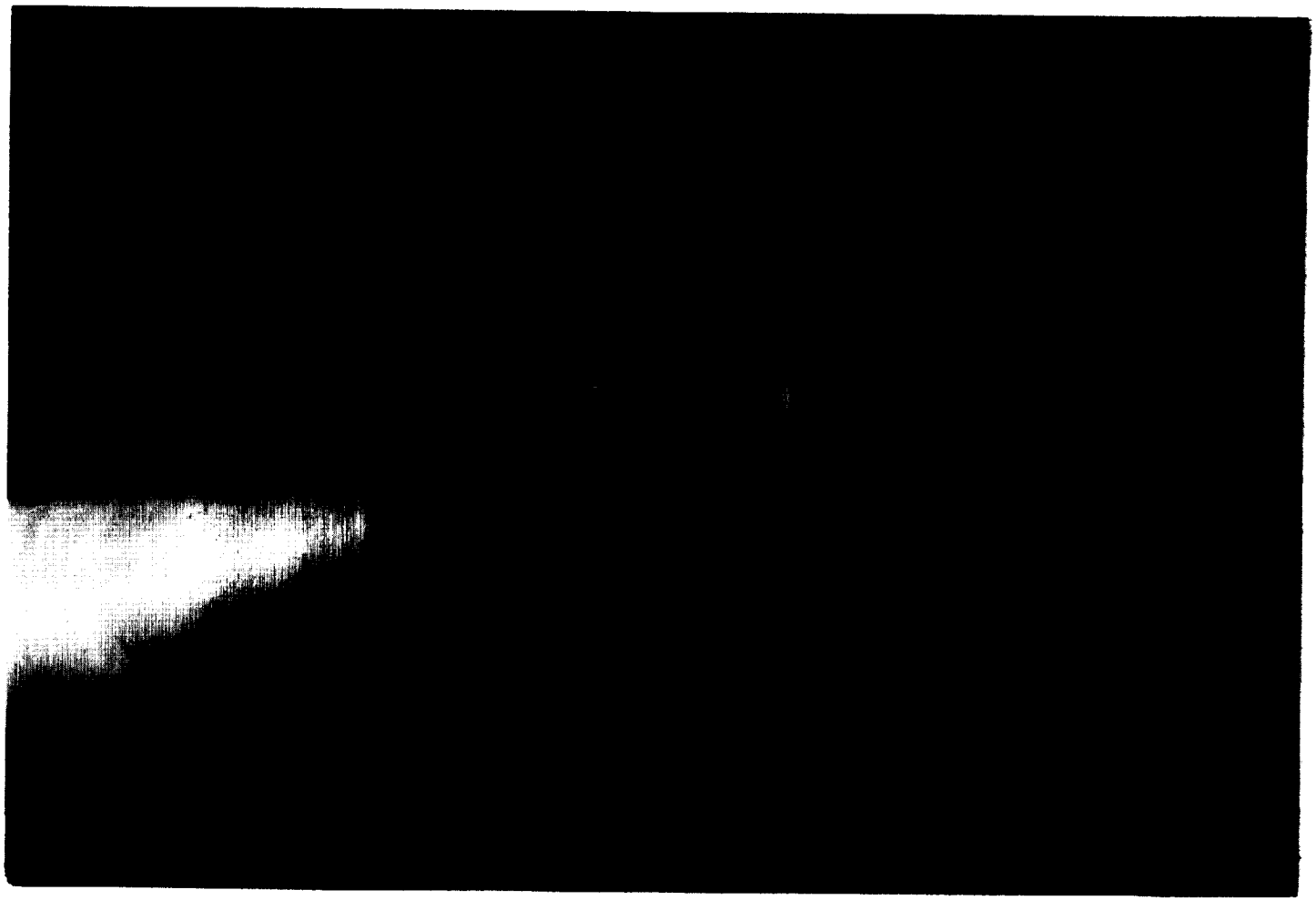

(b) Probe B. L-59-8049

Figure 2.- Continued.

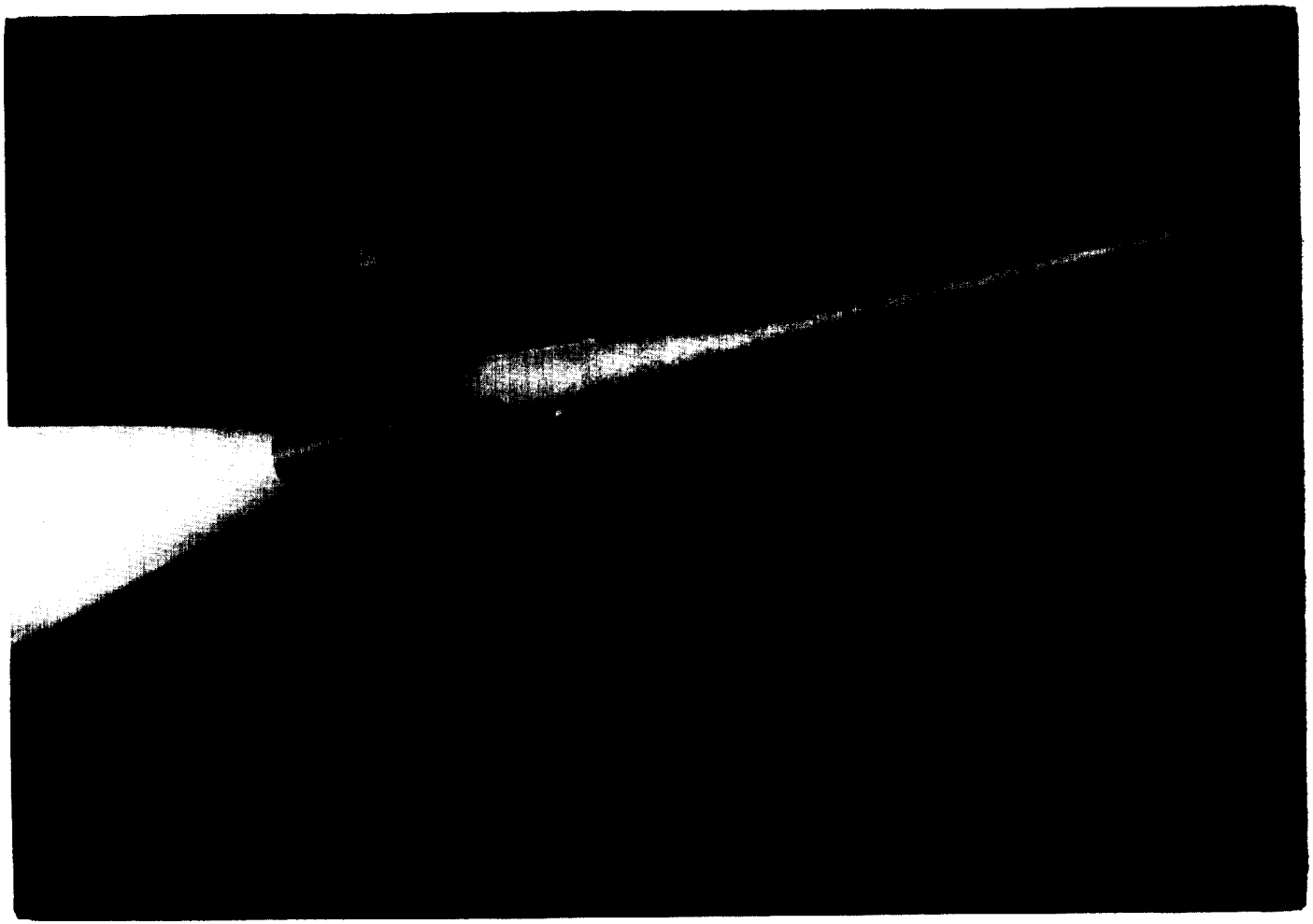

(c) Probe C. L-59-8047

Figure 2.- Continued.

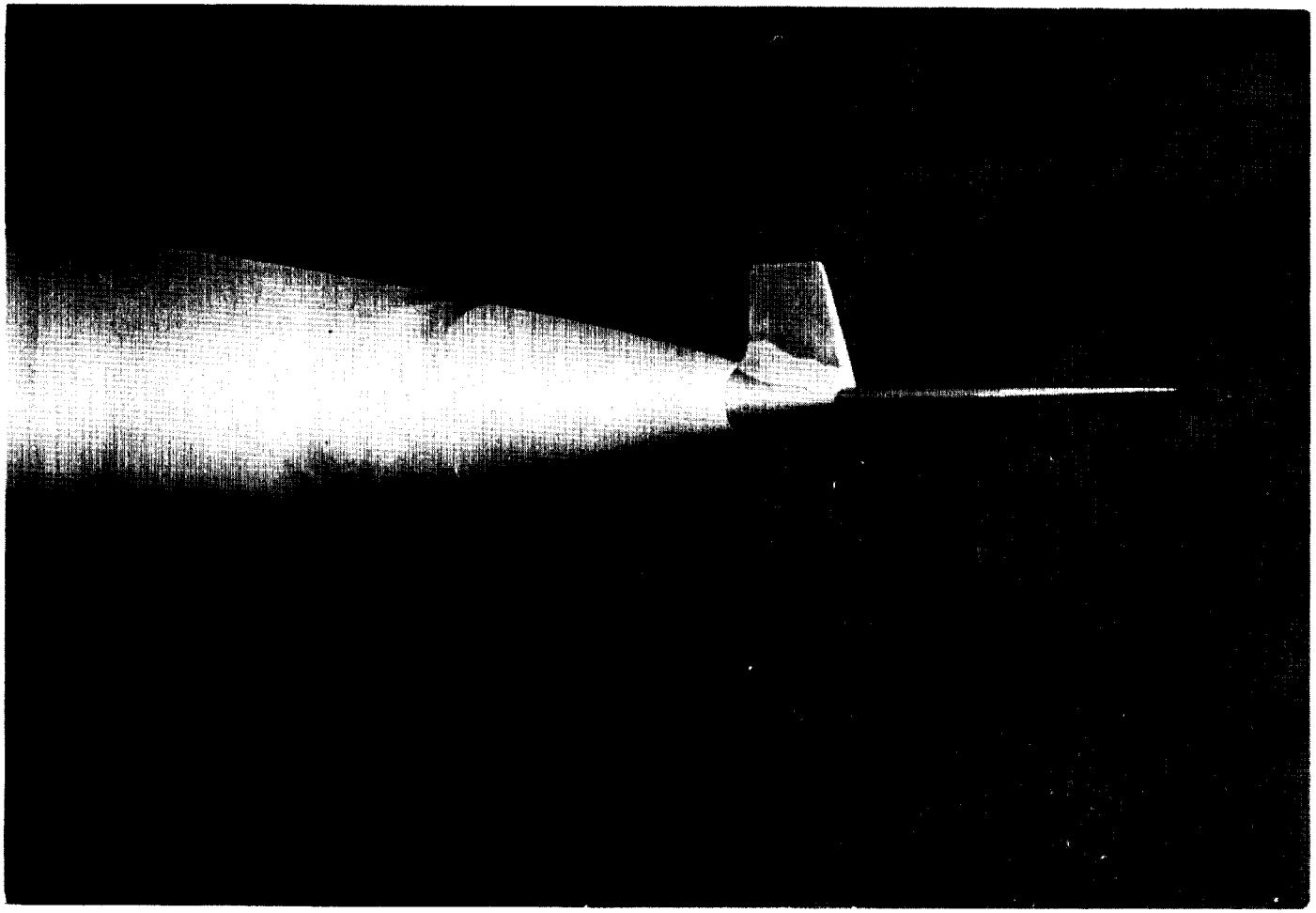

(d) Probe D. L-59-8052

Figure 2.- Continued.

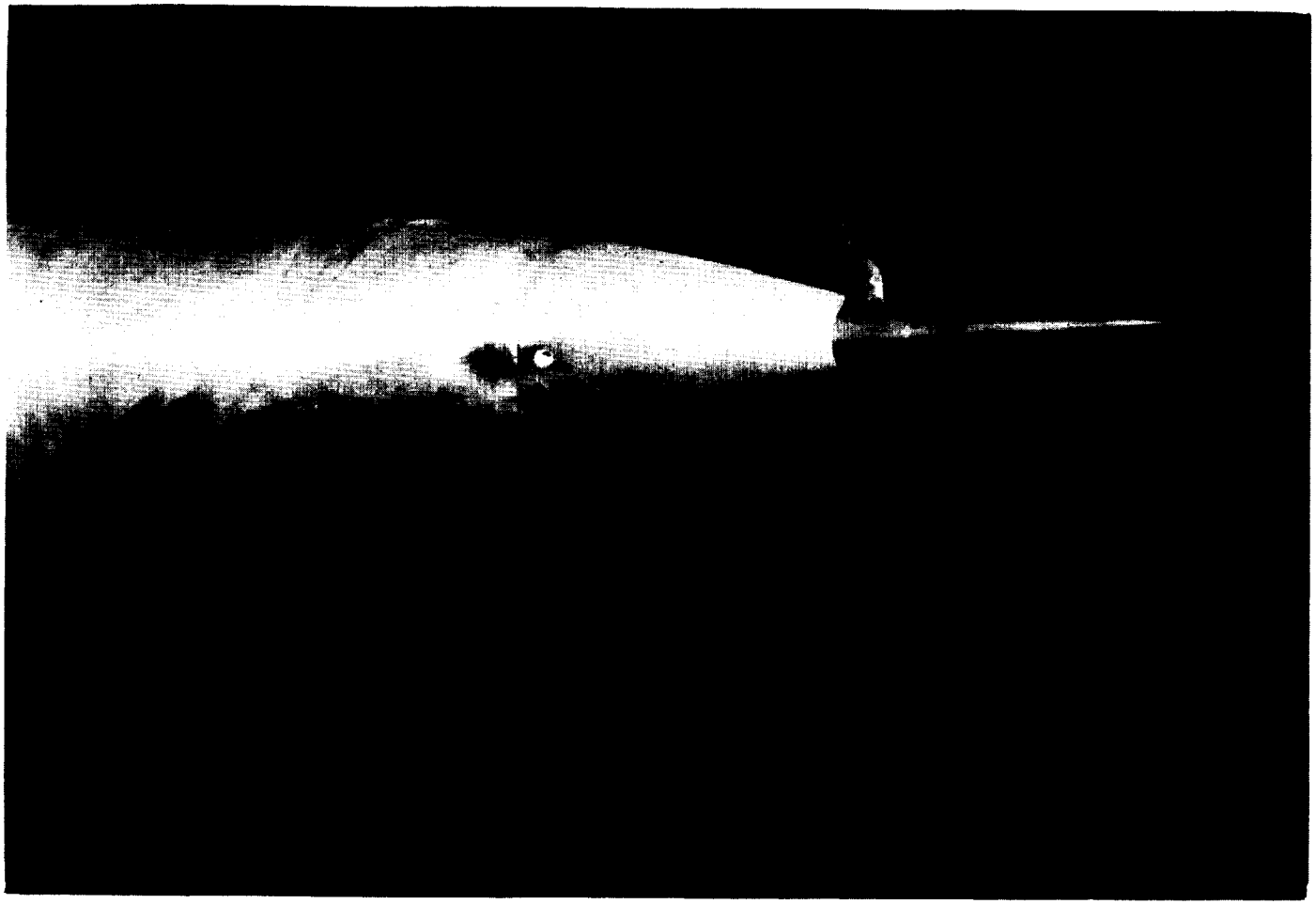

(e) Probe E. L-59-8189

Figure 2.- Continued.

L-59-8050

(f) Probe F.

Figure 2.- Continued.

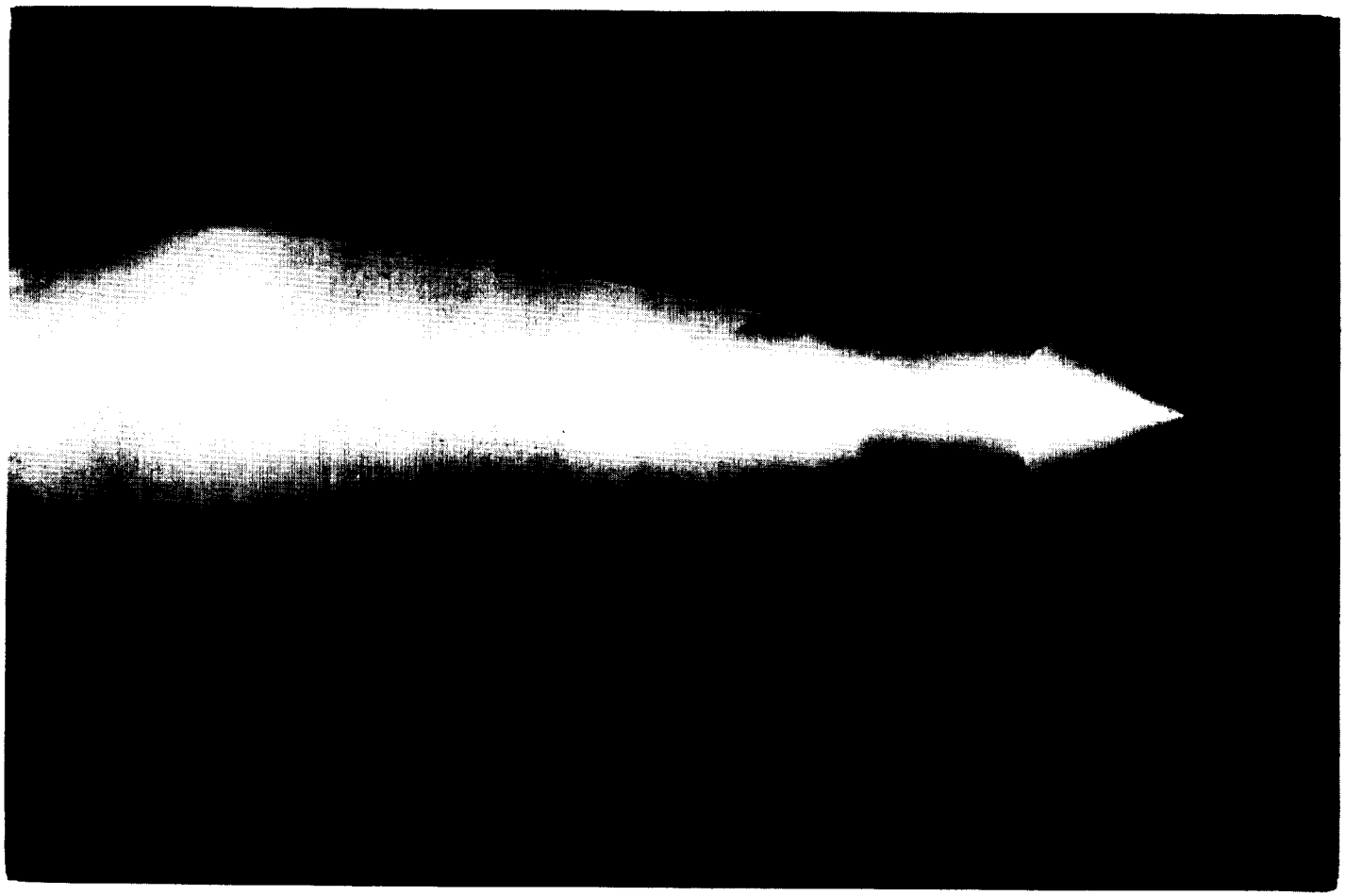

(g) Probe G. L-59-8051

Figure 2.- Concluded.

| Nose Coordinates | |
|---|---|
| x | r |
| 0.00 | 0.00 |
| -0.75 | .31 |
| -2.00 | .66 |
| -3.00 | .89 |
| -4.00 | 1.10 |
| -5.00 | 1.30 |
| -6.00 | 1.49 |

| Body Coordinates | | | |
|---|---|---|---|
| x | r | x | r |
| 0.00 | 0.00 | -50.00 | 7.31 |
| -6.00 | 1.49 | -55.00 | 7.85 |
| -10.00 | 2.19 | -60.00 | 8.37 |
| -15.00 | 2.46 | -65.00 | 8.89 |
| -20.00 | 3.67 | -70.00 | 9.40 |
| -25.00 | 4.34 | -75.00 | 9.90 |
| -30.00 | 4.98 | -80.00 | 10.39 |
| -35.00 | 5.59 | -85.00 | 10.39 |
| -40.00 | 6.18 | -90.00 | 10.39 |
| -45.00 | 6.75 | -94.00 | 10.39 |

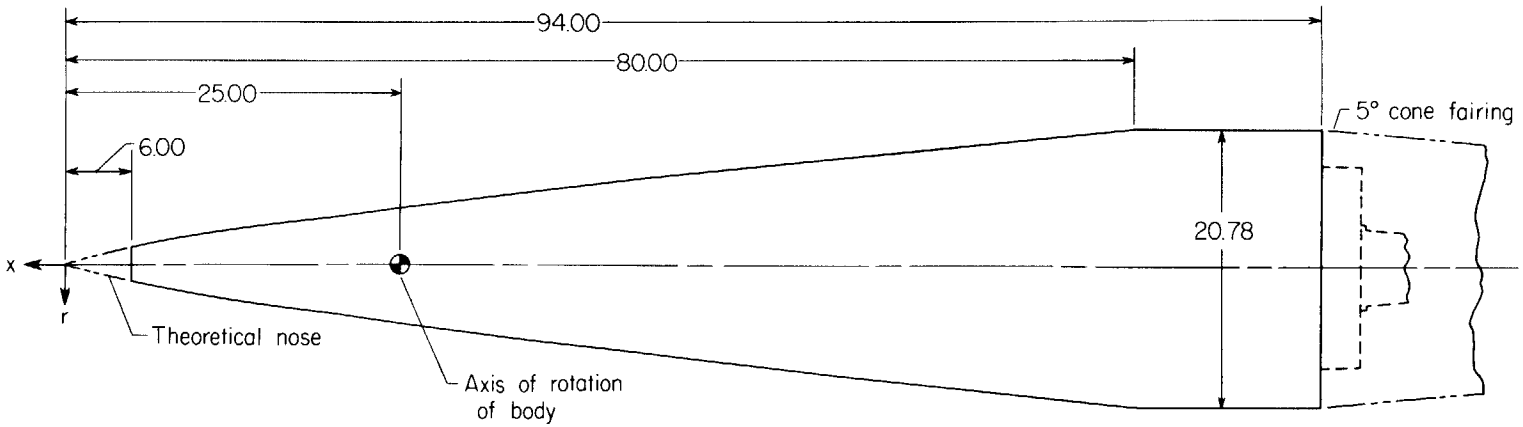


Figure 3.- Sketch of body used for mounting probes. All dimensions are in inches unless otherwise noted.

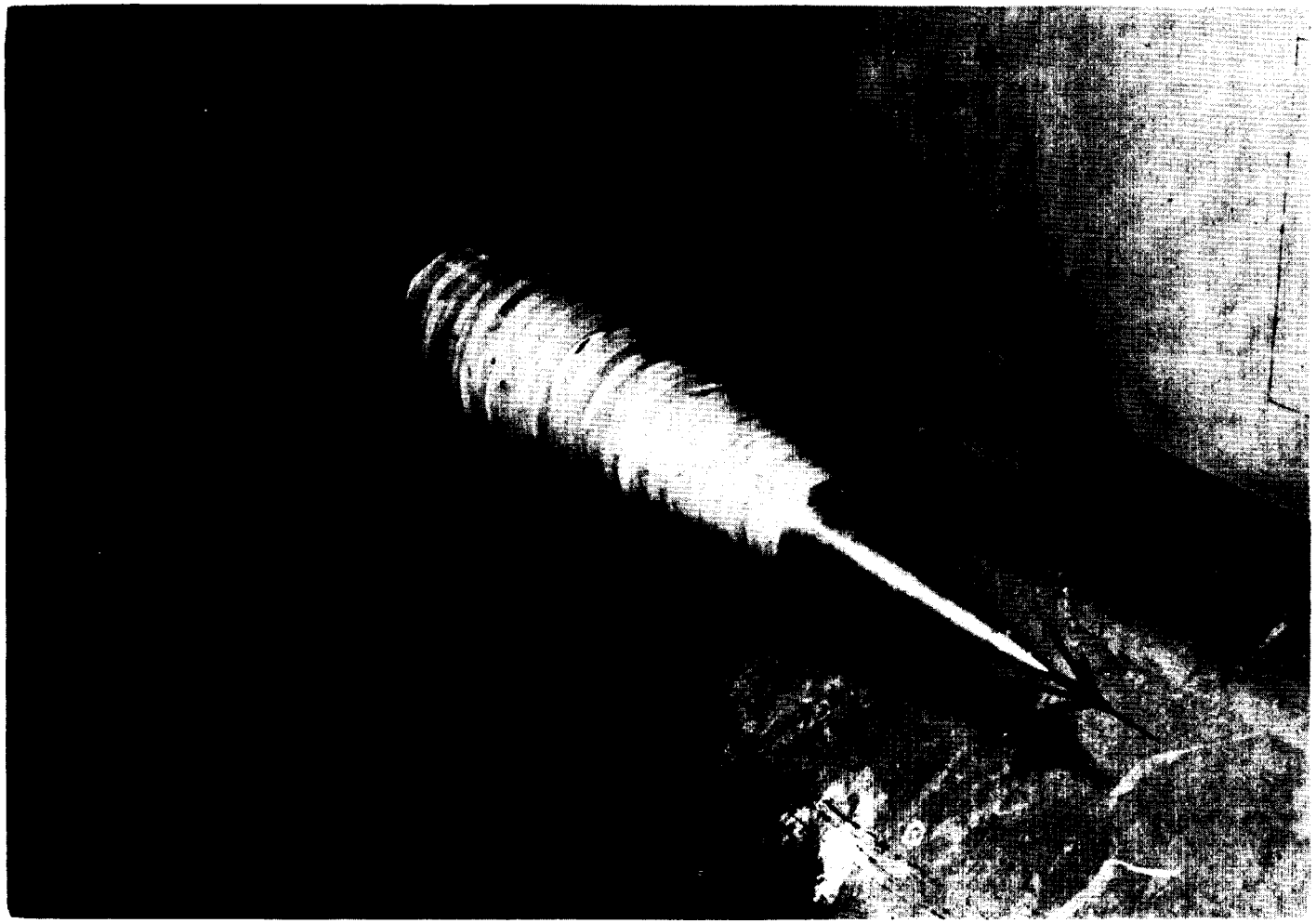

L-59-8045

Figure 4.- Photograph of body with probe C in Langley 16-foot transonic tunnel.

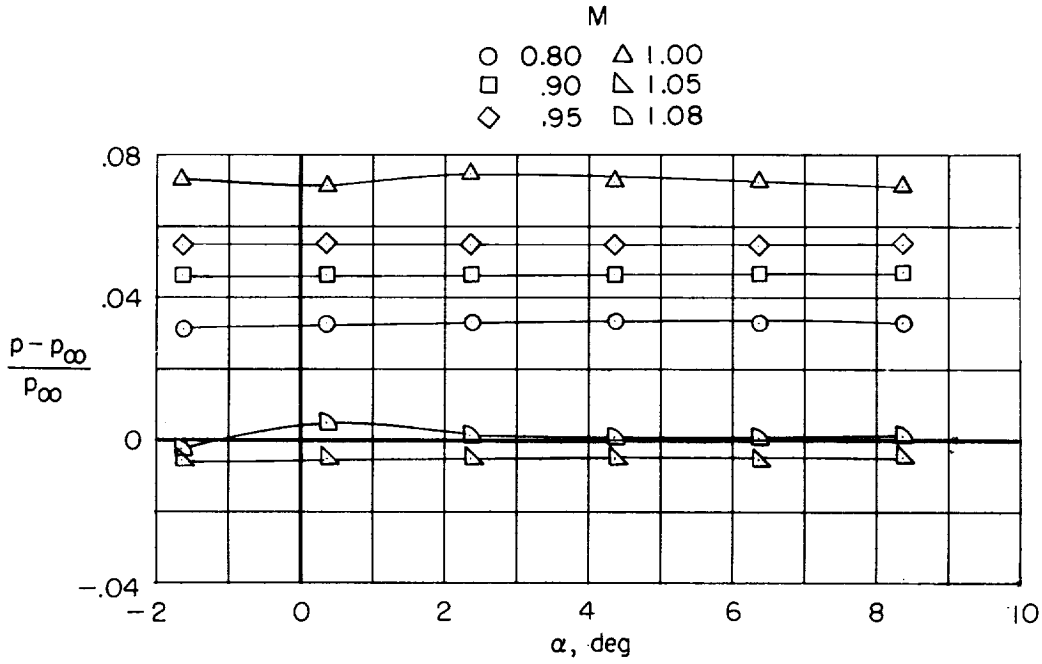


(a) Effect of angle of attack.

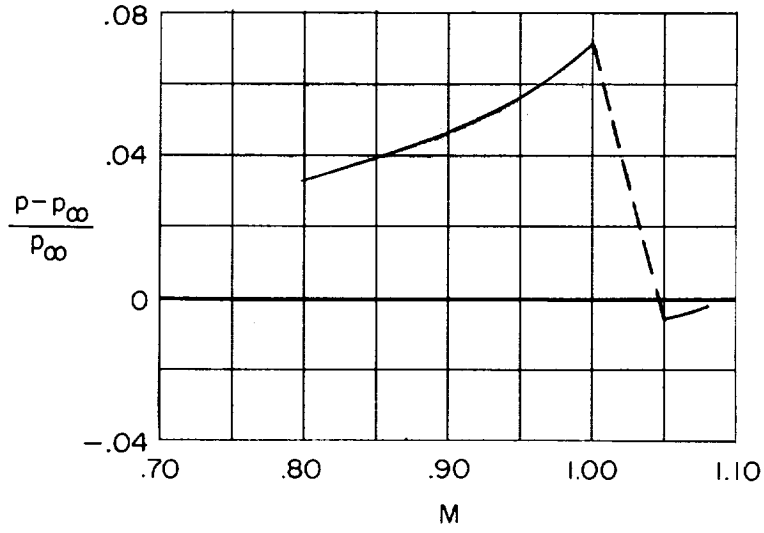


(b) Effect of Mach number at $\alpha = 0^\circ$.

Figure 5.- Variation of static-pressure error coefficient with angle of attack and Mach number for probe A. Dashed lines represent a Mach number range where no data were obtained.

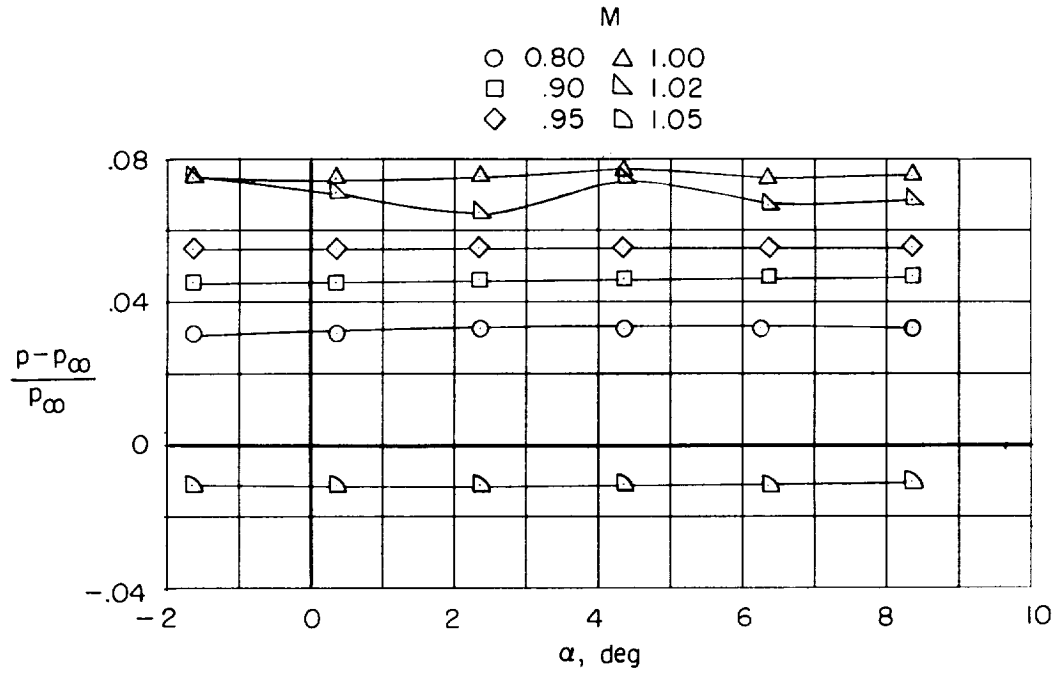


(a) Effect of angle of attack.

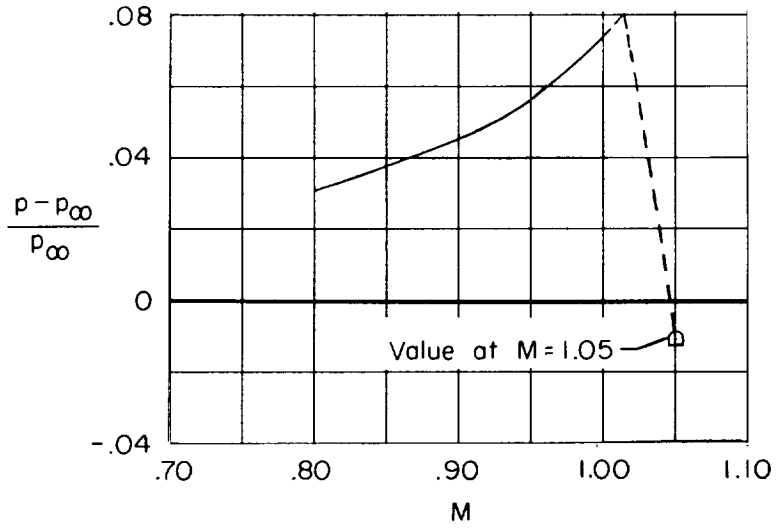


(b) Effect of Mach number at $\alpha = 0^\circ$.

Figure 6.- Variation of static-pressure error coefficient with angle of attack and Mach number for probe B. Dashed lines represent a Mach number range where no data were obtained.

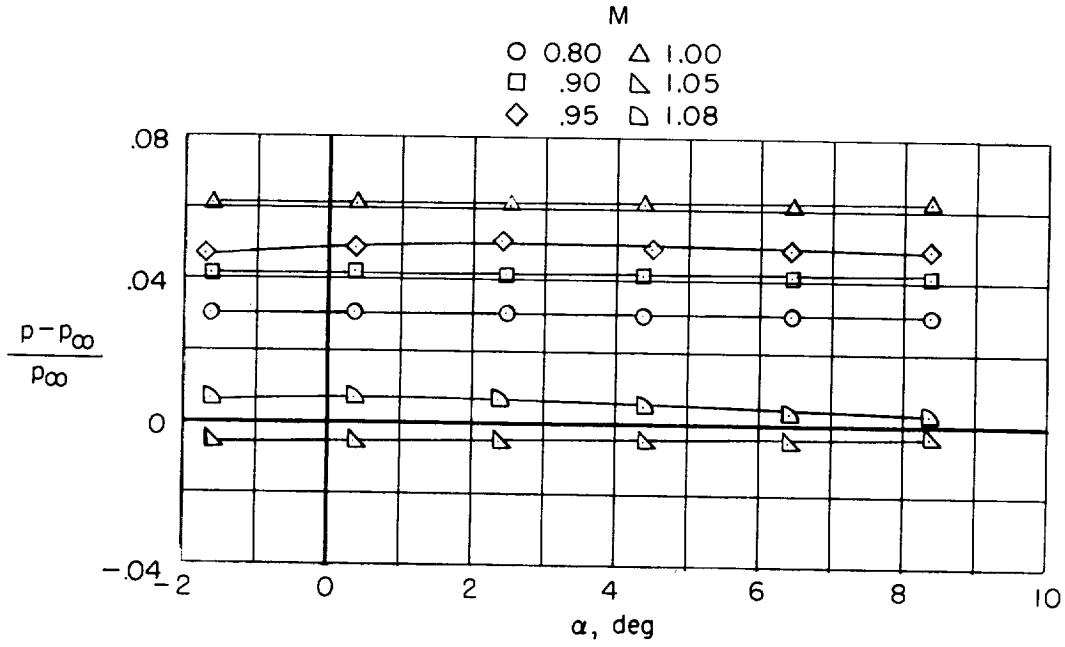


(a) Effect of angle of attack.

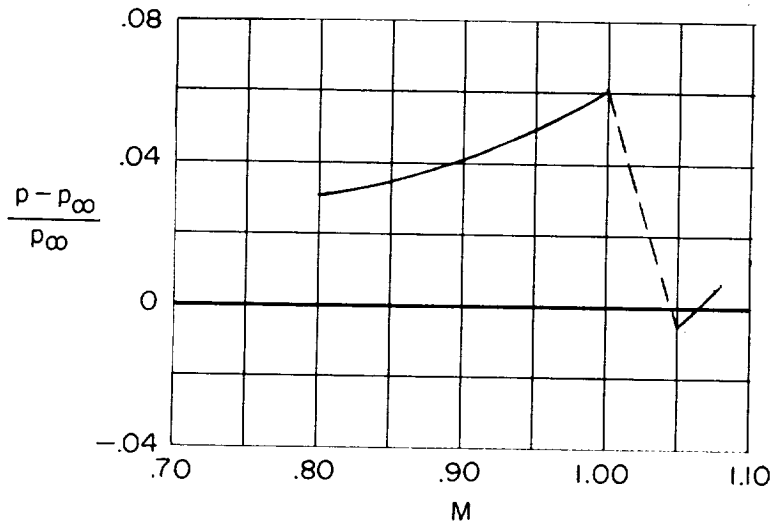


(b) Effect of Mach number at $\alpha = 0^\circ$.

Figure 7.- Variation of static-pressure error coefficient with angle of attack and Mach number for probe C. Dashed lines represent a Mach number range where no data were obtained.

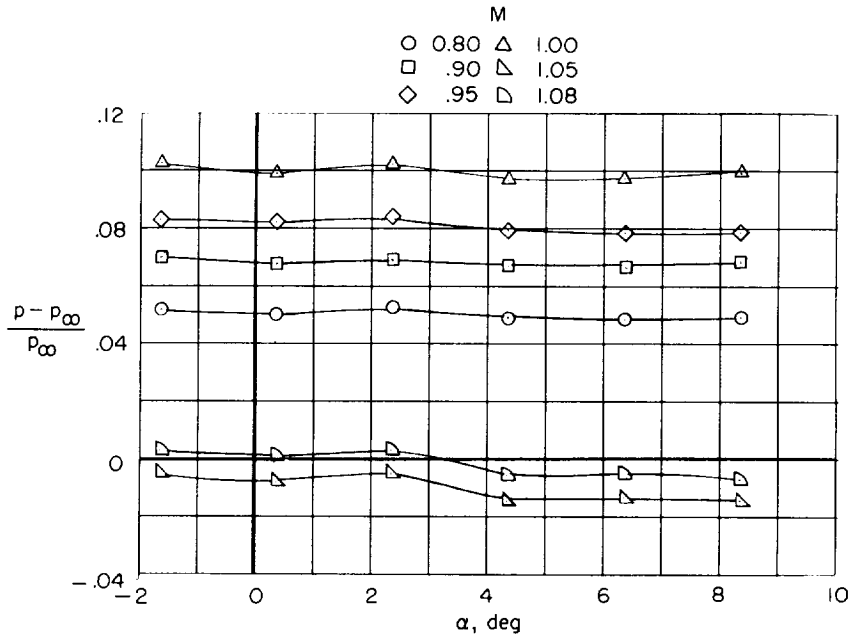


(a) Effect of angle of attack.

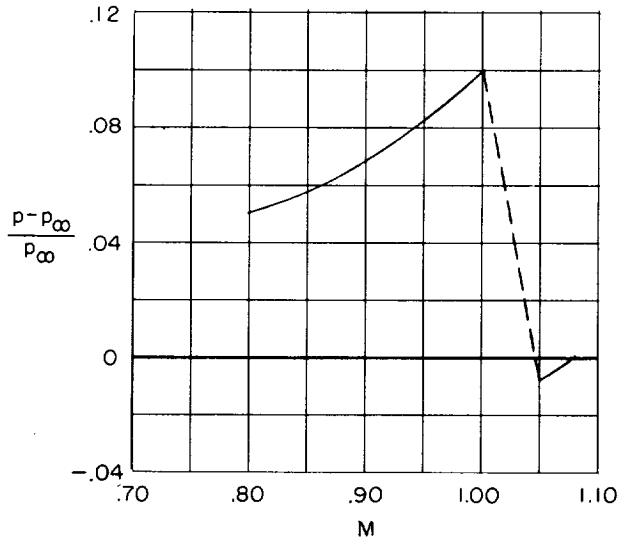


(b) Effect of Mach number at $\alpha = 0^\circ$.

Figure 8.- Variation of static-pressure error coefficient with angle of attack and Mach number for probe D. Dashed lines represent a Mach number range where no data were obtained.

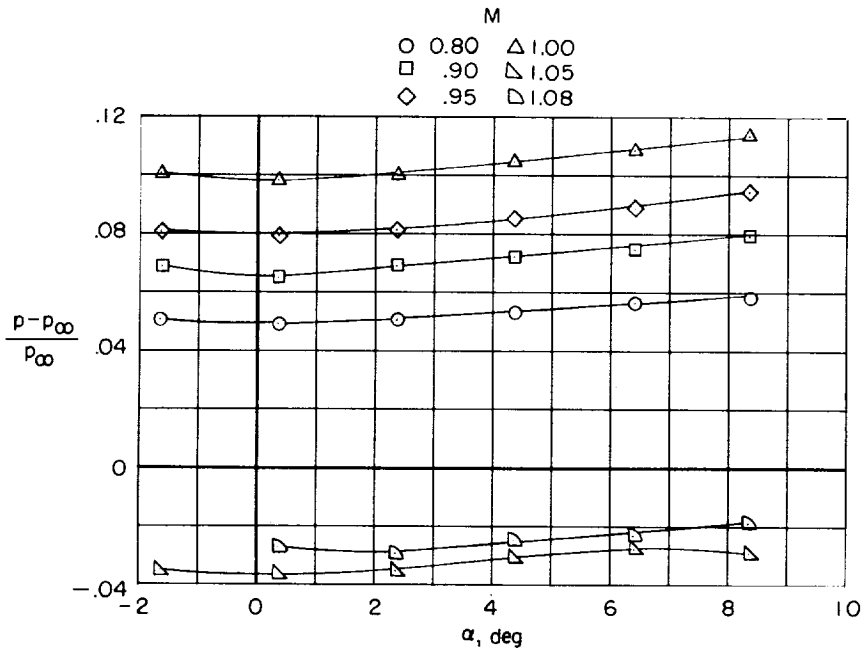


(a) Effect of angle of attack.

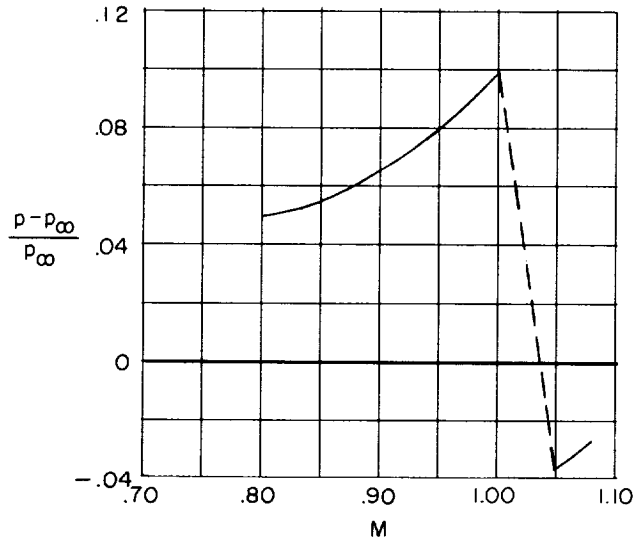


(b) Effect of Mach number at $\alpha = 0^\circ$.

Figure 9.- Variation of static-pressure error coefficient with angle of attack and Mach number for probe E. Dashed lines represent a Mach number range where no data were obtained.

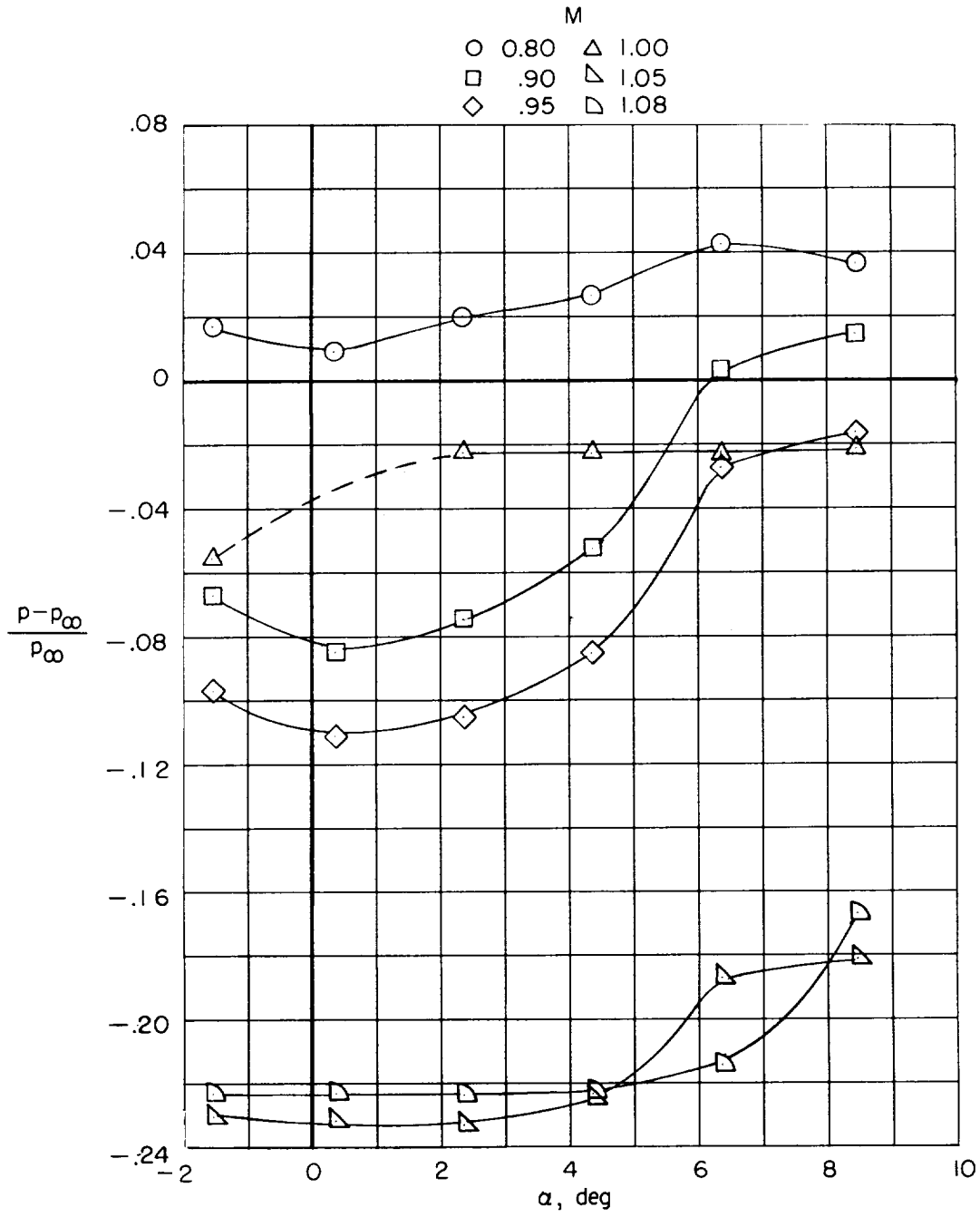


(a) Effect of angle of attack.

Figure 10.- Variation of static-pressure error coefficient with angle of attack and Mach number for probe F. Dashed lines represent a Mach number range where no data were obtained.

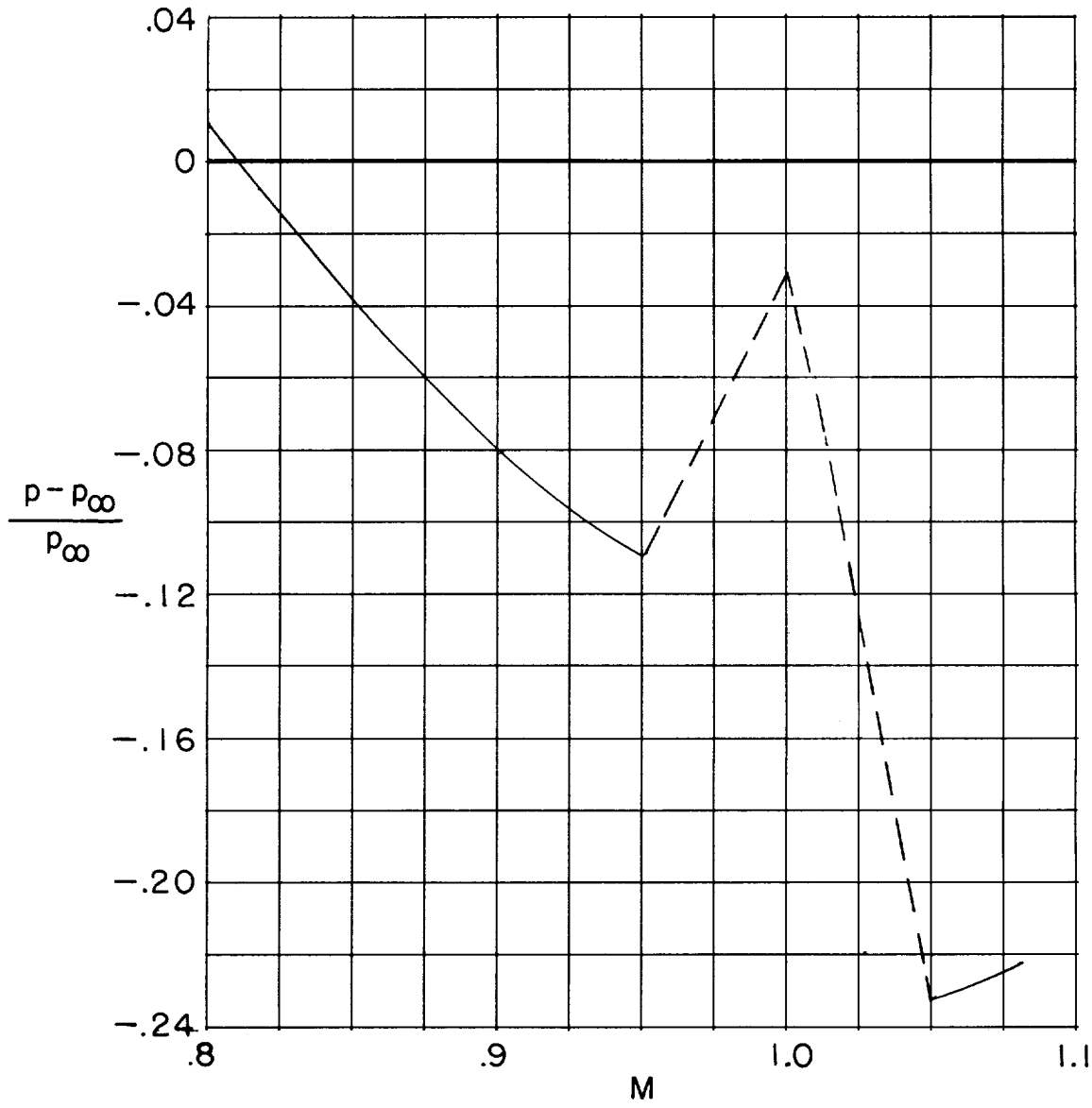


(b) Effect of Mach number at $\alpha = 0^\circ$.

Figure 10.- Concluded.

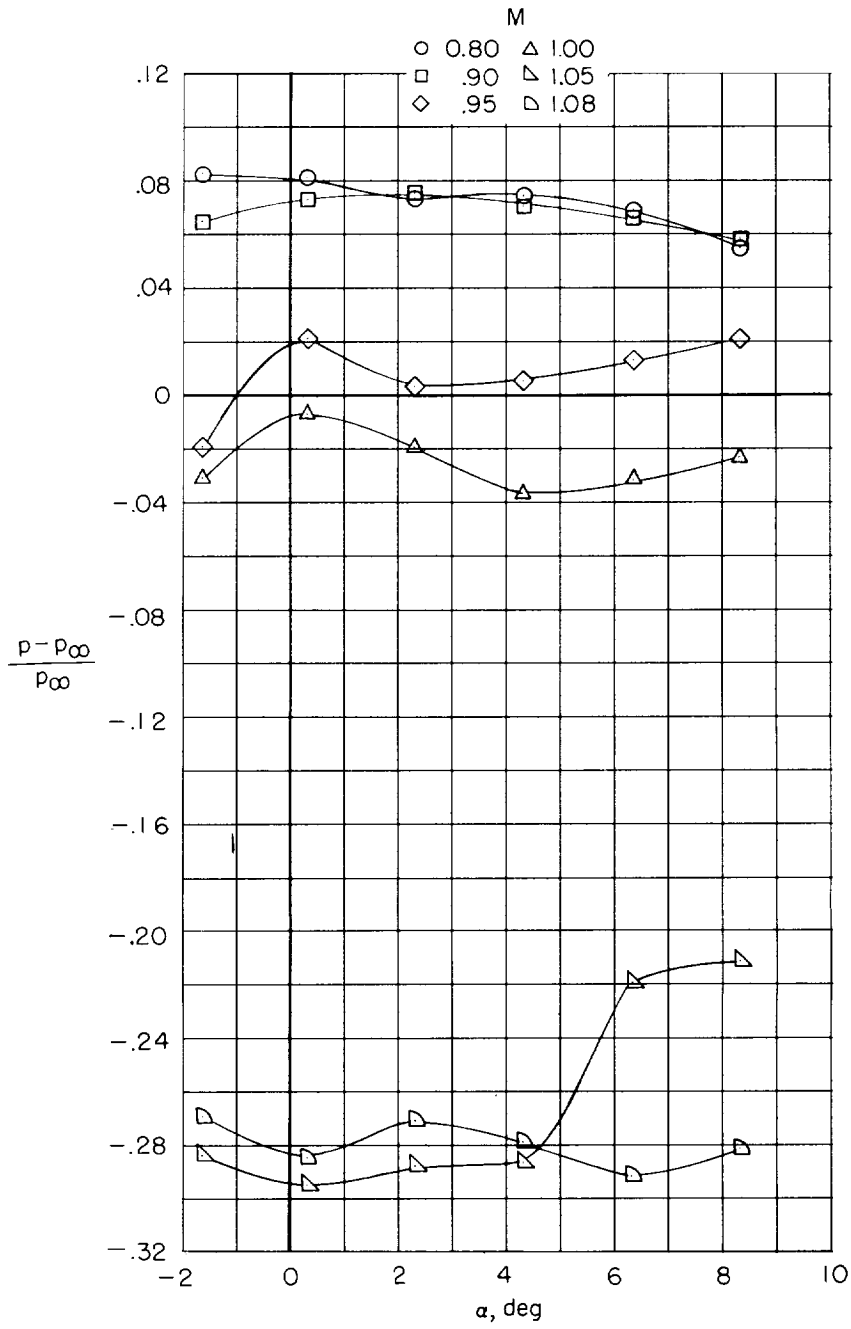


(a) Effect of angle of attack.

Figure 11.- Variation of static-pressure error coefficient with angle of attack and Mach number for probe G. Dashed lines represent a Mach number range where no data were obtained.

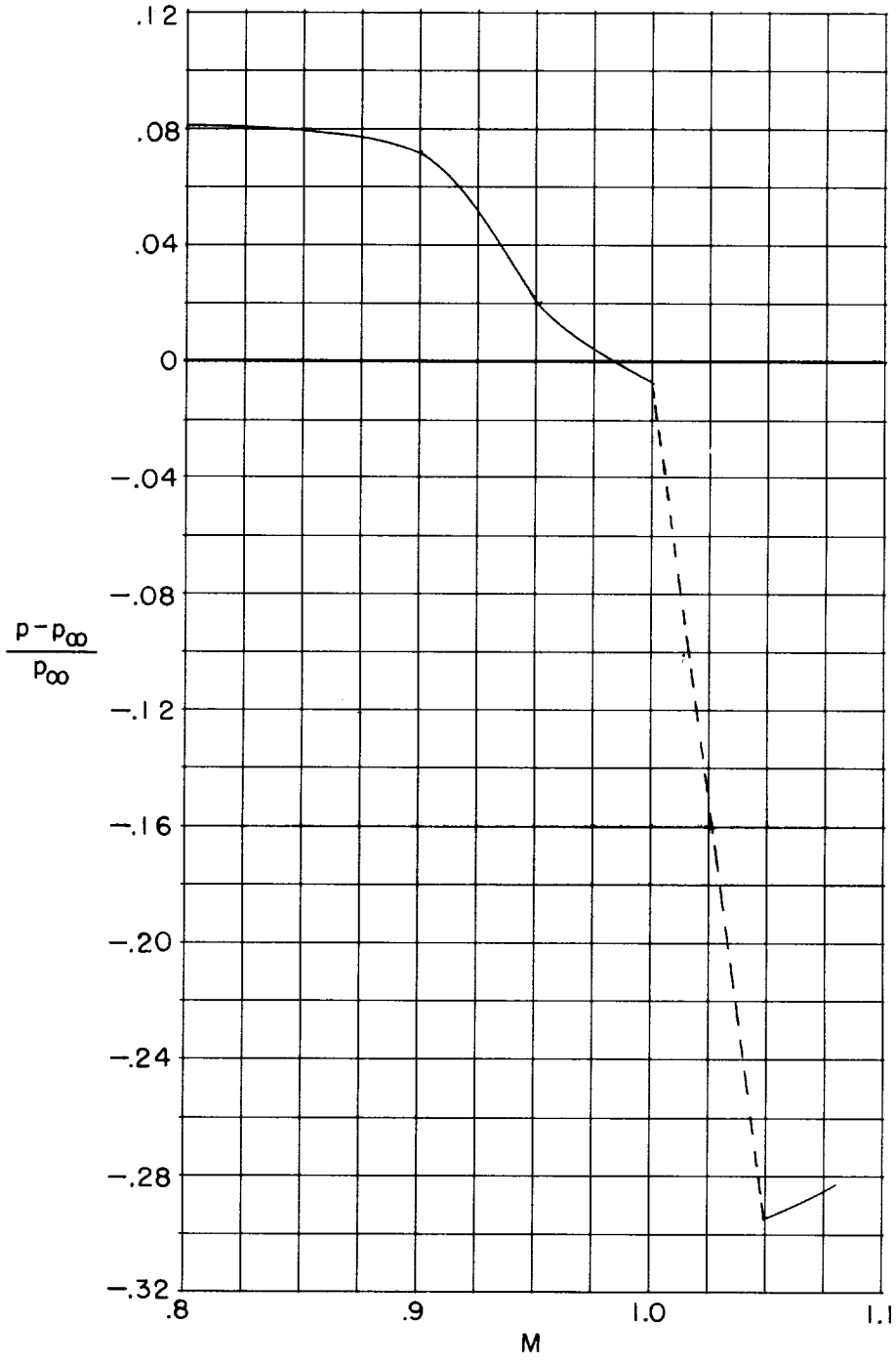


(b) Effect of Mach number at $\alpha = 0^\circ$.

Figure 11.- Concluded.

NASA-Langley, 1961 L-1563

NASA TN D-947
National Aeronautics and Space Administration.
WIND-TUNNEL TESTS OF SEVEN STATIC-PRESSURE PROBES AT TRANSONIC SPEEDS.
Francis J. Capone. November 1961. 30p. OTS price, $0.75. (NASA TECHNICAL NOTE D-947)

The errors of seven static-pressure probes mounted very close to the nose of a body of revolution were determined at Mach numbers from 0.80 to 1.08 and at angles of attack from -1.7° to 8.4°. Three of the probes were equipped with a gimbal system and four vanes that alined the probe with the local flow. Two single-vane, self-rotating probes had two orifices at ±37.5° from the plane of symmetry on the lower surface of the probe. Two probes were fixed, cone-cylinder probes of short length and large diameter.

Copies obtainable from NASA, Washington

I. Capone, Francis J.
II. NASA TN D-947

(Initial NASA distribution:
1, Aerodynamics, aircraft;
2, Aerodynamics, missiles and space vehicles.)

NASA

NASA TN D-947
National Aeronautics and Space Administration.
WIND-TUNNEL TESTS OF SEVEN STATIC-PRESSURE PROBES AT TRANSONIC SPEEDS.
Francis J. Capone. November 1961. 30p. OTS price, $0.75. (NASA TECHNICAL NOTE D-947)

The errors of seven static-pressure probes mounted very close to the nose of a body of revolution were determined at Mach numbers from 0.80 to 1.08 and at angles of attack from -1.7° to 8.4°. Three of the probes were equipped with a gimbal system and four vanes that alined the probe with the local flow. Two single-vane, self-rotating probes had two orifices at ±37.5° from the plane of symmetry on the lower surface of the probe. Two probes were fixed, cone-cylinder probes of short length and large diameter.

Copies obtainable from NASA, Washington

I. Capone, Francis J.
II. NASA TN D-947

(Initial NASA distribution:
1, Aerodynamics, aircraft;
2, Aerodynamics, missiles and space vehicles.)

NASA

NASA TN D-947
National Aeronautics and Space Administration.
WIND-TUNNEL TESTS OF SEVEN STATIC-PRESSURE PROBES AT TRANSONIC SPEEDS.
Francis J. Capone. November 1961. 30p. OTS price, $0.75. (NASA TECHNICAL NOTE D-947)

The errors of seven static-pressure probes mounted very close to the nose of a body of revolution were determined at Mach numbers from 0.80 to 1.08 and at angles of attack from -1.7° to 8.4°. Three of the probes were equipped with a gimbal system and four vanes that alined the probe with the local flow. Two single-vane, self-rotating probes had two orifices at ±37.5° from the plane of symmetry on the lower surface of the probe. Two probes were fixed, cone-cylinder probes of short length and large diameter.

Copies obtainable from NASA, Washington

I. Capone, Francis J.
II. NASA TN D-947

(Initial NASA distribution:
1, Aerodynamics, aircraft;
2, Aerodynamics, missiles and space vehicles.)

NASA

NASA TN D-947
National Aeronautics and Space Administration.
WIND-TUNNEL TESTS OF SEVEN STATIC-PRESSURE PROBES AT TRANSONIC SPEEDS.
Francis J. Capone. November 1961. 30p. OTS price, $0.75. (NASA TECHNICAL NOTE D-947)

The errors of seven static-pressure probes mounted very close to the nose of a body of revolution were determined at Mach numbers from 0.80 to 1.08 and at angles of attack from -1.7° to 8.4°. Three of the probes were equipped with a gimbal system and four vanes that alined the probe with the local flow. Two single-vane, self-rotating probes had two orifices at ±37.5° from the plane of symmetry on the lower surface of the probe. Two probes were fixed, cone-cylinder probes of short length and large diameter.

Copies obtainable from NASA, Washington

I. Capone, Francis J.
II. NASA TN D-947

(Initial NASA distribution:
1, Aerodynamics, aircraft;
2, Aerodynamics, missiles and space vehicles.)

NASA